

Tumor-Selective Radiopharmaceutical Targeting via Receptor-Mediated Endocytosis of Gallium-67-Deferoxamine-Folate

Carla J. Mathias, Susan Wang, Robert J. Lee, David J. Waters, Philip S. Low and Mark A. Green

Departments of Chemistry, Veterinary Clinical Sciences and Medicinal Chemistry, Purdue University, West Lafayette, Indiana

The receptor-mediated endocytosis uptake pathway for the vitamin folate was investigated as a target for tumor-selective radiopharmaceutical delivery. The molecular target for this delivery mechanism is a membrane-associated folate binding protein (FBP) that is overexpressed by a variety of malignant cell lines. **Methods:** The ability of a ^{67}Ga -labeled deferoxamine-folate conjugate (^{67}Ga -DF-folate) to target tumor cells in vivo was examined using an athymic mouse tumor model. Subcutaneous inoculation of $\sim 4 \times 10^6$ folate-receptor-positive KB (human nasopharyngeal carcinoma) cells into athymic mice yielded ~ 0.20 g tumors in 15 days, at which time either ^{67}Ga -DF-folate, ^{67}Ga -deferoxamine (^{67}Ga -DF) or ^{67}Ga -citrate was administered by intravenous injection. **Results:** The ^{67}Ga -DF-folate conjugate showed marked tumor-specific deposition in vivo, with $1.0 \pm 0.3\%$ of the injected dose (%ID) in tumor at 4 hr postinjection (equating to 5.2 ± 1.5 %ID/g tumor; $n = 3$ mice). Corresponding tumor-to-background ratios at 4 hr postinjection were: tumor/blood = 409 ± 195 ; tumor/muscle = 124 ± 47 ; tumor/liver = 11 ± 3 ; and tumor/kidney = 2.6 ± 0.9 . Tumor uptake of ^{67}Ga -DF-folate conjugate was effectively blocked by co-injection of 2.4 ± 1.0 mg free folate. In control experiments, ^{67}Ga -citrate exhibited tumor uptake of $2.2 \pm 0.4\%$ of the injected dose (10.9 ± 0.2 %ID/g tumor), but very poor target-to-background contrast (tumor/blood = 0.84 ± 0.19 ; tumor/muscle = 5.4 ± 0.7 ; tumor/liver = 2.3 ± 0.2 ; and tumor/kidney = 2.4 ± 0.3). Unconjugated ^{67}Ga -deferoxamine showed no tumor affinity. **Conclusion:** Receptor-mediated endocytosis of radiolabeled folate-conjugates may offer a suitable mechanism for selectively delivering radiopharmaceuticals to tumors for diagnostic imaging and/or radiation therapy.

Key Words: gallium-67; folate binding protein; tumor imaging; receptor-mediated endocytosis

J Nucl Med 1996; 37:1003-1008

Receptor-mediated endocytosis (1-5) is an attractive mechanism for cell-selective drug targeting, since this process exhibits high transport capacity, as well as ligand-dependent cell specificity. In cultured cells it is well established that receptor-mediated endocytosis of folate-conjugates can be employed to achieve tumor cell-selective uptake of a wide variety of exogenous molecules that are normally excluded from the cell (6-12). Folic acid is an essential dietary vitamin used by all eucaryotic cells for DNA synthesis and one-carbon metabolism. Folic acid primarily enters cells through facilitated transport by a membrane transport protein ($K_m = 1.5 \times 10^{-6}$ M for folic acid) (13-16). Some cells also possess a membrane-associated folate-receptor, folate binding protein (FBP), that additionally

allows folate uptake via endocytosis ($K_a \approx 5 \times 10^{-10}$ M for folate) (1,4). When folate is covalently conjugated to macromolecules or liposomes via its gamma-carboxylate, the folate moiety is no longer recognized by the facilitated transport system, but can still be recognized by the folate binding protein (6-12). Thus, such folate-conjugates are selectively concentrated by cells that express the membrane folate receptor.

A number of tumor cell types (e.g., breast, ovarian, cervical, colorectal, renal and nasopharyngeal) are known to overexpress FBP (17-27). Such neoplasms would appear to be good candidates for tumor-selective radiopharmaceutical targeting via folate receptor-mediated endocytosis. Folate binding protein is so dramatically overexpressed in many tumors that this receptor has already been exploited in vitro as a marker to localize and visualize tumor cells (13-25). In fact, FBP has even been found to be the antigen target for a number of tumor-specific monoclonal antibodies (17-19,22,25,28).

We report here an investigation of tumor-selective radiopharmaceutical targeting using a ^{67}Ga -deferoxamine-folate conjugate (^{67}Ga -DF-folate) (Fig. 1). The animal model employed for these drug-targeting studies was the athymic mouse subcutaneously implanted with human nasopharyngeal carcinoma (KB) cells known to overexpress FBP. Previously, we have shown that the ^{67}Ga -deferoxamine-folate conjugate exhibits saturable FBP receptor-mediated uptake into these KB cells in vitro (29).

EXPERIMENTAL PROCEDURES

General

The deferoxamine-folate (γ) conjugate (DF-folate) (Fig. 1) was prepared as described elsewhere (29). A radionuclide dose calibrator was used for assays of ^{67}Ga radioactivity in the μCi -mCi range; while low level (<0.01 μCi) samples of ^{67}Ga were counted in an automatic gamma scintillation counter with a 3-inch large-bore NaI(Tl) crystal. Gamma images of intact animals were obtained using a gamma scintillation camera fitted with a 300-keV parallel-hole collimator and linked to a computer. Folate-deficient rodent chow was obtained commercially and autoclaved prior to use. All animal experiments were carried out in accordance with procedures approved by the Purdue Animal Care and Use Committee.

Preparation of the Gallium-67 Radiotracers

The ^{67}Ga -deferoxamine-folate conjugate, ^{67}Ga -citrate and ^{67}Ga -deferoxamine were prepared, as described elsewhere (29), from no-carrier-added ^{67}Ga -gallium(III) chloride. Briefly, a dilute HCl solution of $^{67}\text{Ga}^{3+}$ was evaporated to dryness with heating under a stream of N_2 and the tracer reconstituted in ~ 300 μl ethanol containing 0.002% acetylacetone (acac). The ethanolic $^{67}\text{Ga}(\text{acac})_3$ solution (3.2 mCi) was diluted with an equal volume of TRIS-

Received June 5, 1995; revision accepted Oct. 18, 1995.

For correspondence or reprints contact: Mark A. Green, PhD, Department of Medicinal Chemistry, Purdue University, 1333 Pharmacy Bldg., West Lafayette, IN 47907-1333.

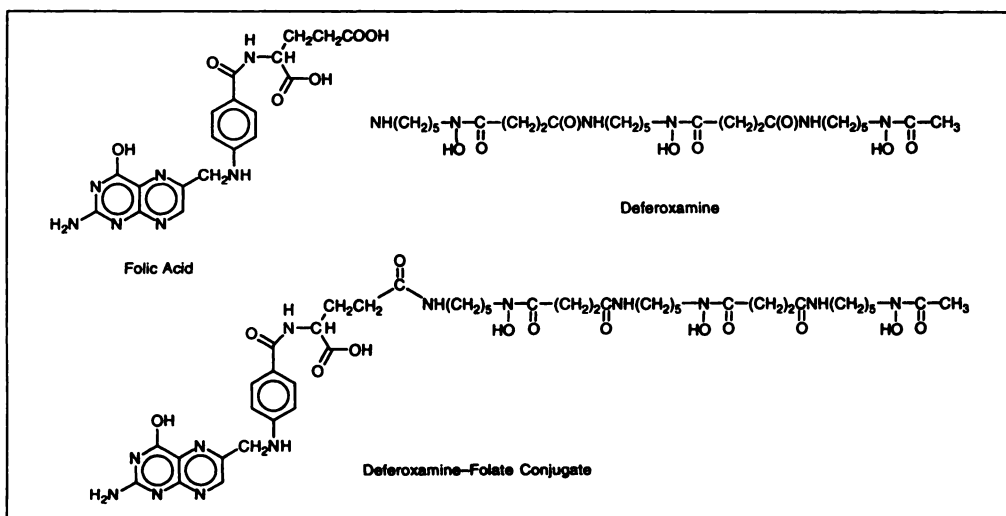


FIGURE 1. Chemical structures of folic acid, deferoxamine and the deferoxamine-folate conjugate.

buffered saline (pH 7.4) (30) followed by addition of 2.25×10^{-6} mole of aqueous DF-folate (γ) conjugate. Labeling was complete after standing at room temperature for 18–24 hr. For control experiments $^{67}\text{Ga}(\text{III})$ -citrate was prepared by evaporating a ^{67}Ga -chloride solution to dryness and reconstituting with 0.1 ml of 3% sodium citrate (pH 7.4). A portion of the resulting ^{67}Ga -citrate solution (50 μl) was mixed with 0.1 mg deferoxamine to obtain ^{67}Ga -deferoxamine (^{67}Ga -DF) for control experiments. The radiochemical purity of each ^{67}Ga -labeled compound was determined by thin layer chromatography on C_{18} reverse phase silica gel plates developed with methanol and in all cases was found to exceed 98% at the time of use. The radiochromatograms were evaluated using a Berthold (Wildbad, Germany) Tracemaster 20 Automatic TLC Linear Analyzer. R_f values of 0.93; 0.0; 0.1; and 0.74 were obtained for ^{67}Ga -DF-folate (γ); $^{67}\text{Ga}(\text{acac})_3$; ^{67}Ga -DF; and ^{67}Ga -citrate, respectively. All experiments employing the ^{67}Ga -DF-folate (γ) tracer were performed within 1–3 days of radiolabeling.

Growth and Preparation of KB Cells

KB cells, a human nasopharyngeal epidermal carcinoma cell line that greatly overexpresses the folate binding protein (31), were cultured in a 75 cm^2 flask continuously as a monolayer at 37°C in a humidified atmosphere containing 5% CO_2 . A folate-deficient modified Eagle's medium (FDMEM) was used (a folate-free modified Eagle's medium purchased from Gibco (Grand Island, NY) supplemented with 10% v/v heat-inactivated fetal calf serum as the only source of folate) containing penicillin (50 units/ml), streptomycin (50 $\mu\text{g}/\text{ml}$) and 2 mM L-glutamine. The final folate concentration in the complete FDMEM is ~ 3 nM, i.e., a value at the low end of the physiological concentration in human serum (13,32). To prepare for implantation, KB cells were transferred into 225 cm^2 flasks and grown in FDMEM until confluent. At this point the cells were harvested by treating with trypsin (140 USP U/ml) and EDTA (0.07 mM) in buffer A (136.9 mM NaCl, 2.68 mM KCl, 8.1 mM Na_2HPO_4 , 1.47 mM KH_2PO_4 and phenol red). The cells were then washed once with FDMEM and pelleted by spinning at $1000 \times G$ for 3 to 5 min. The cell pellet was resuspended at 4×10^6 cells per 0.4 ml in FDMEM.

Athymic Mouse Tumor Model

Four- to 5-wk-old male athymic mice (nu/nu strain) were used. All food, water and bedding were sterilized prior to use. Mice were housed under conditions of controlled temperature ($72 \pm 2^\circ\text{F}$) and humidity in polycarbonate cages using a microisolator system. Daily light cycles were 12 hr light, 12 hr dark. After a 7-day acclimation period 17 mice were inoculated subcutaneously with 0.1 ml of tumor cell suspension (4×10^6 KB cells) into the

interscapular region using a 25-gauge needle. All inoculations were performed within a laminar flow cabinet using aseptic technique. Subcutaneous tumor growth was monitored daily and radiotracer distribution studies performed 9 to 15 days after tumor cell implantation when tumors reached approximately 50 mm^3 (0.008–0.28 g). Unless otherwise indicated, animals used in the reported biodistribution experiments were exclusively fed folate-free rodent chow ad libitum for 2–3 wk prior to radiopharmaceutical administration.

Mouse Serum Folate Concentrations

Blood was collected from three athymic mice receiving regular (folate-supplemented) rodent chow and 1, 2 and 3 wk after diet was changed to folate-free rodent chow. In each instance blood was collected by left ventricular puncture using a 27-gauge needle. Blood samples were centrifuged and serum collected and frozen at -70°C until assay for folate concentrations.

Serum folate was determined using a ligand binding competition assay. Briefly, KB cells were plated in 35-mm culture dishes and grown to $\sim 80\%$ confluence in FDMEM. The cells were then washed with ice-cold phosphate-buffered saline (PBS; 136.9 mM NaCl, 2.68 mM KCl, 8.1 mM Na_2HPO_4 , 1.47 mM KH_2PO_4 , pH 7.4) and 100 pmole of [^3H]-folic acid added in 1 ml folate-free medium (free folates were removed by dialysis) in the absence or presence of 50 μl mouse serum. After 30 min incubation at 4°C, the cells were washed with 3×1 ml cold PBS and suspended in PBS by scraping. The cell-associated radioactivity was determined by scintillation counting and cellular protein content evaluated using the BCA (bicinchoninic acid) protein assay kit. The folate concentration in mouse serum was calculated by the following equation:

Serum folate (nM)

$$= \frac{100 \text{ pmole} \times (\text{CPM}_o \text{ per cell} - \text{CPM}_i \text{ per cell})}{(\text{CPM}_i \text{ per cell}) \times 0.05 \text{ ml}}$$

where CPM_o is the cell-associated radioactivity with 100 pmole [^3H]-folic acid alone and CPM_i is the cell-associated radiotracer in the presence of 50 μl mouse serum.

Imaging and Radiotracer Biodistribution Studies

Animals were anesthetized with ketamine (40 mg/kg, intraperitoneally) and xylazine (4 mg/kg, intraperitoneally) for radiopharmaceutical injection, for gamma imaging studies and again prior to death. Syringes used for radiotracer injections were weighed on

TABLE 1
Biodistribution of Gallium-67 Radiotracers in Athymic Mice with Subcutaneous KB Cell Tumors

| | %ID/g of tissue 4 hr after intravenous administration* | | | | | |
|-----------------|--|---------------|-------------|---------------|---------------------|--------------------------|
| | ⁶⁷ Ga-DF-Folate† | | | | ⁶⁷ Ga-DF | ⁶⁷ Ga-citrate |
| | Group 1 | Group 2 | Group 3 | Group 4‡ | Group 5 | Group 6 |
| Blood | 0.014 ± 0.004 | 0.019 ± 0.011 | 0.45 ± 0.16 | 0.046 ± 0.009 | 0.026 ± 0.009 | 13.5 ± 3.2 |
| Heart | 0.029 ± 0.004 | 0.024 ± 0.014 | 0.17 ± 0.05 | 0.025 ± 0.005 | 0.021 ± 0.002 | 3.4 ± 0.2 |
| Lungs | 0.038 ± 0.005 | 0.063 ± 0.001 | 0.38 ± 0.14 | 0.052 ± 0.010 | 0.054 ± 0.010 | 9.1 ± 2.7 |
| Liver | 0.46 ± 0.08 | 0.40 ± 0.16 | 0.87 ± 0.18 | 0.43 ± 0.03 | 0.082 ± 0.010 | 4.7 ± 0.3 |
| Kidney | 2.02 ± 0.32 | 3.5 ± 1.8 | 24.3 ± 1.6 | 1.79 ± 0.82 | 1.26 ± 0.19 | 4.6 ± 0.4 |
| Muscle | 0.044 ± 0.006 | 0.029 ± 0.023 | 0.13 ± 0.06 | 0.028 ± 0.005 | 0.037 ± 0.001 | 2.04 ± 0.29 |
| Tumor | 5.2 ± 1.5 | 1.0 ± 0.29 | 0.26 ± 0.09 | 2.22 ± 0.36 | 0.094 ± 0.004 | 10.9 ± 0.2 |
| Tumor mass (g) | 0.21 ± 0.07 | 0.20 ± 0.02 | 0.11 ± 0.07 | 0.22 ± 0.02 | 0.13 ± 0.09 | 0.20 ± 0.03 |
| Animal mass (g) | 28.1 ± 1.1 | 25.6 ± 2.5 | 27.9 ± 2.7 | 28.3 ± 0.6 | 27.8 ± 2.3 | 27.6 ± 2.0 |

*Values shown represent the mean ± s.d. of data from three animals (n = 2 for Group 2).

†Group 2—mice on normal (folate-rich) diet; Group 3—folate receptor blocked with preadministration of folate; Group 4—folate chase intravenously 3.5 hr following ⁶⁷Ga-DF-folate administration.

‡Animals killed 4.5 hr (rather than 4 hr) following ⁶⁷Ga-DF-folate administration.

an analytical balance before and after injection to quantitate the dose received by each animal.

In a pilot study to test the viability of the FBP-receptor as a pathway for achieving tumor-cell-selective uptake of metal-labeled radiopharmaceuticals *in vivo*, ~180 μCi ⁶⁷Ga-deferoxamine-folate conjugate were administered intravenously to each of two tumor-bearing athymic mice via the femoral vein nine days after subcutaneous inoculation with 4 × 10⁶ KB cells and 15 days after initiation of folate-free diet. At 46 hr postinjection a lethal dose of ketamine/xylazine was administered to one animal, a 0.1-ml blood sample collected by cardiac puncture, and a 100,000-count static gamma image acquired to visualize the tissue distribution of radiotracer. The second animal was sacrificed at 45 hr post-⁶⁷Ga-DF-folate administration. The tissues identified in Table 1 were collected and, after radioactivity in the weighed tissue samples decayed to a suitable ⁶⁷Ga count rate, the tissue distribution of tracer was quantitated by gamma counting.

A series of 18 additional mice was studied 15 days after subcutaneous inoculation with 4 × 10⁶ human KB cells into the interscapular region. Each animal received 125–150 μCi of ⁶⁷Ga-DF-folate (12 mice; Groups 1–4), or ⁶⁷Ga-DF (3 mice; Group 5), or ⁶⁷Ga-citrate (3 mice; Group 6) via intravenous injection into the femoral vein. Injection volumes were ~130 μl of 10% ethanol in saline per animal. All animals except three were maintained on folate-deficient diet for 22 days prior to radiotracer administration; the remaining three animals were maintained on normal rodent chow and included in the animals that received ⁶⁷Ga-DF-folate (Group 2; one animal in Group 2 died after initial administration of anesthesia, generating no data). To competitively block tumor folate receptors, three mice received 2.4 ± 1.0 mg folate intravenously ~5 min prior to ⁶⁷Ga-DF-folate administration (Group 3). Three different mice that received ⁶⁷Ga-DF-folate also received 3.5 ± 0.9 mg of folate intravenously approximately 1 hr before being sacrificed (Group 4). The tissue distribution of the tracers was monitored by gamma scintigraphy at approximately 15 min, 1 hr and 3 hr postinjection to qualitatively assess tumor uptake of tracer and tumor/background contrast. At 4–4.5 hr following administration of the ⁶⁷Ga-radiopharmaceuticals, the anesthetized animals were sacrificed by decapitation and the tumor and selected tissues removed, weighed and stored until ⁶⁷Ga had decayed to levels suitable for counting. The biodistribution of tracer in each sample was calculated as both a percentage of the injected dose per organ (%ID/organ) and as a percentage of the injected dose per

gram of tissue wet weight (%ID/g), using counts from a weighed and appropriately diluted sample of the original injectate for reference. Tumor/nontarget tissue ratios were calculated from the corresponding %ID/g values. A one-tailed Mann-Whitney test (33) was used to assess the significance of differences in radiotracer tumor uptake between the animals in Group 1 and the animals in Groups 2, 3 and 4.

RESULTS

To create an animal model suitable for evaluation of folate-receptor targeting *in vivo*, athymic mice were implanted subcutaneously with ~4 × 10⁶ human nasopharyngeal carcinoma (KB) cells previously used in the study of folate-receptor targeting *in vitro* (29). Measurable tumors consistently developed 7–10 days after cell implantation. Upon section at the time of study the tumors had negligible degree of necrosis.

Since normal rodent chow contains a high concentration of folic acid (6 mg/kg chow), unless otherwise indicated the mice used in the tumor-targeting studies were maintained on folate-free diet to achieve serum folate concentrations closer to the 4–6 μg/l (9–14 nM) range of normal human serum (32). Figure 2 shows the measured mouse serum folate levels as a function

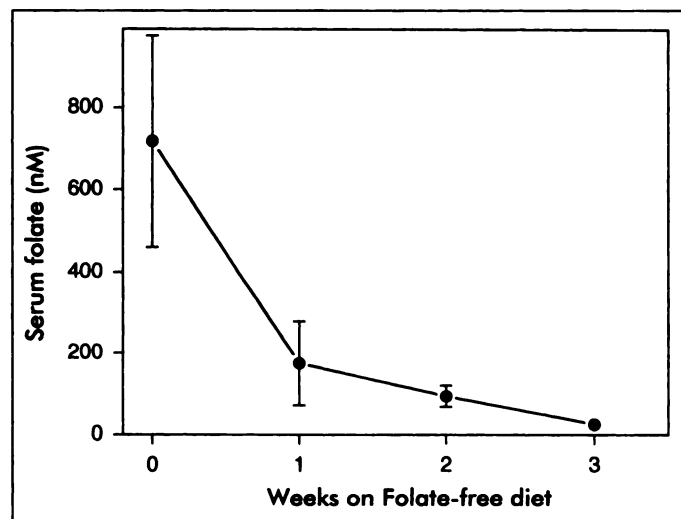
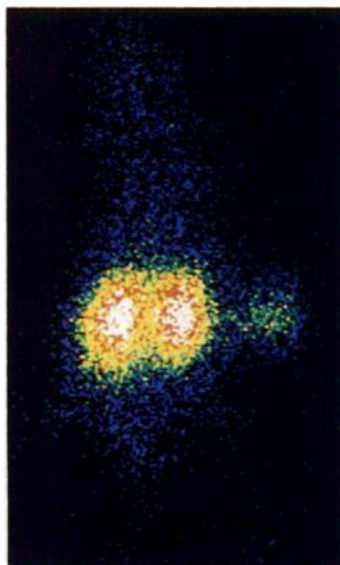


FIGURE 2. Variation of serum folate concentrations after placing athymic mice on a folate-deficient diet. For reference, the concentration of folic acid in normal human serum is 4–6 μg/l (9–14 nM) (32).

FIGURE 3. Gamma image obtained 46 hr following intravenous administration of ^{67}Ga -deferoxamine-folate conjugate to a male athymic mouse bearing a KB tumor (implanted subcutaneously on the left side of the abdomen). In this dorsal view the mouse is oriented nose up with the mouse's left to the reader's right. The kidneys are responsible for the most intense (white-yellow) spots in the abdominal region. The yellow-green spot on the right is the tumor.



of time following initiation of the folate-deficient diet. In most of the present radiopharmaceutical-targeting studies animals were used 3 wk after initiation of the folate-free diet, a time when mouse serum folate levels were found to be $25 \pm 7 \text{ nM}$ (Fig. 2).

In a pilot study to test the viability of the folate-receptor as a pathway for tumor-cell-selective uptake of metal-labeled radiopharmaceuticals in vivo, $\sim 180 \mu\text{Ci}$ of ^{67}Ga -deferoxamine-folate conjugate was administered intravenously to each of two tumor-bearing athymic mice that had been maintained on folate-free diet for 2 wk. At ~ 45 hr postinjection, gamma images were obtained, the animals killed and the tissue distribution of ^{67}Ga quantitated. The tumors from these two animals were found to have masses of 29.6 and 8 mg, while the total body mass of these animals was 19.3 and 22.6 g, respectively. Despite the small size and suboptimal positioning of these tumors relative to the kidneys, the 29.6-mg tumor was readily detected by gamma scintigraphy (Fig. 3). At death, the 29.6-mg tumor contained 3.3% of the injected dose per gram of tumor. Relevant tumor-to-background ratios (%ID/g) for this animal were: tumor-to-blood = 1600; tumor-to-muscle = 170; tumor-to-liver = 59; and tumor-to-kidney = 2.4. The distribution of tracer was similar in the second animal with the 8-mg tumor, where we found 2.8% ID/g tumor with corresponding tumor-to-nontarget ratios of: tumor-to-blood = 1200; tumor-to-muscle = 290; tumor-to-liver = 92; and tumor-to-kidney = 2.7.

To better define the ability of ^{67}Ga -DF-folate to target tumor cells in vivo and to confirm the role of the folate receptor in

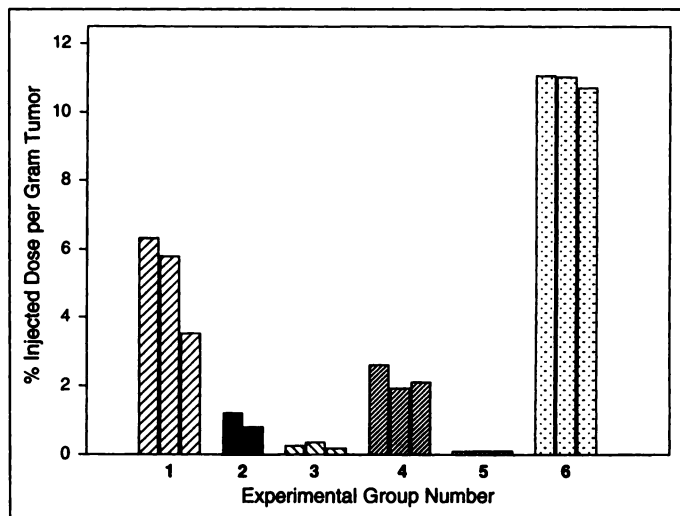


FIGURE 4. Tumor uptake of ^{67}Ga radiotracers 4-4.5 hr following intravenous administration. Each bar represents the data from one animal. Group 1— ^{67}Ga -DF-folate; Group 2— ^{67}Ga -DF-folate in mice on high-folate diet; Group 3— ^{67}Ga -DF-folate administered with excess folic acid; Group 4— ^{67}Ga -DF-folate with chase dose of folate intravenously 1 hr prior to sacrifice; Group 5— ^{67}Ga -DF; Group 6— ^{67}Ga -citrate.

determining conjugate tumor uptake, a series of 17 additional mice was studied after generation of subcutaneous KB cell tumors in the interscapular region. Fifteen of these animals were placed on folate-free diet for 3 wk prior to study, while the remaining two animals were fed normal rodent chow. Gamma scintigraphy provided a convenient means of qualitatively monitoring the tissue distribution of ^{67}Ga following intravenous injection of ^{67}Ga -DF-folate; tumor uptake was evident at 1 hr postinjection, and by ~ 3 hr postinjection the tracer initially present in the liver had substantially cleared into the intestines. A chase dose of folate was administered intravenously to three of the animals at 3.5 hr (Group 4) and all the mice sacrificed at 4 or 4.5 hr after ^{67}Ga injection for quantitative evaluation of tracer biodistribution. Tables 1 and 2 present a summary of the biodistribution data for the ^{67}Ga -labeled deferoxamine-folate conjugate, plus the ^{67}Ga -Df and ^{67}Ga -citrate reference tracers. For each animal studied in this experiment, the tumor uptake of ^{67}Ga is shown in Figure 4, while Figure 5 shows the corresponding tumor-to-blood ratios.

The tumor targeting obtained with ^{67}Ga -DF-folate, ^{67}Ga -DF and ^{67}Ga -citrate was reasonably reproducible within the groups of mice, while clear variations are apparent between groups (Figs. 4, 5 and Tables 1 and 2). The ^{67}Ga -DF-folate tracer was found to significantly concentrate in these folate-receptor-

TABLE 2
Tumor-to-Background Tissue Contrast Obtained with Gallium-67 Radiotracers in the Athymic Mouse Model

| | Tumor-to-nontarget ratio 4 hr after intravenous administration of radiotracer* | | | | | |
|--------------|--|-------------|---------------|-----------|----------------------|---------------------------|
| | ^{67}Ga -DF-folate† | | | | ^{67}Ga -DF | ^{67}Ga -citrate |
| | Group 1 | Group 2 | Group 3 | Group 4‡ | Group 5 | Group 6 |
| Tumor/Blood | 409 ± 195 | 60 ± 18 | 0.64 ± 0.31 | 48 ± 5 | 3.9 ± 1.2 | 0.84 ± 0.19 |
| Tumor/Muscle | 124 ± 47 | 44 ± 24 | 2.3 ± 1.2 | 82 ± 16 | 2.56 ± 0.15 | 5.4 ± 0.7 |
| Tumor/Liver | 11.4 ± 3.2 | 2.5 ± 0.3 | 0.29 ± 0.07 | 5.1 ± 0.5 | 1.16 ± 0.10 | 2.3 ± 0.2 |
| Tumor/Kidney | 2.6 ± 0.9 | 0.31 ± 0.08 | 0.011 ± 0.004 | 1.4 ± 0.5 | 0.08 ± 0.01 | 2.4 ± 0.3 |

*Values shown represent the mean ± s.d. of data from three animals (n = 2 for Group 2).

†Group 2—mice on normal (folate-rich) diet; Group 3—folate receptor blocked with preadministration of folate; Group 4—folate chase intravenously 3.5 hr following ^{67}Ga -DF-folate administration.

‡Animals killed 4.5 hr (rather than 4 hr) after ^{67}Ga -DF-folate administration.

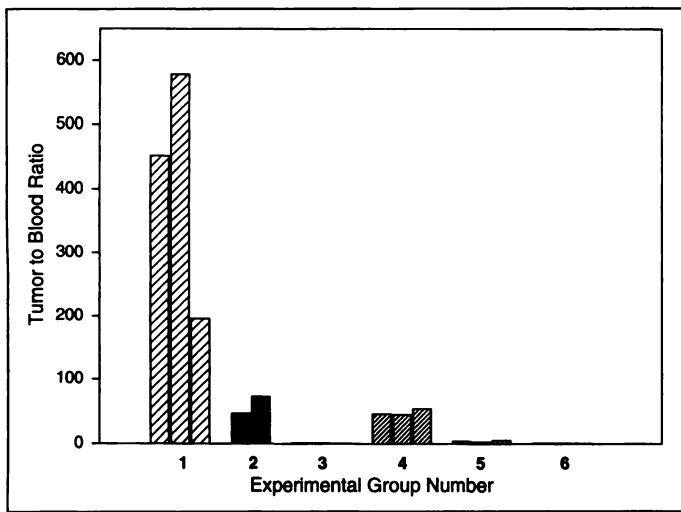


FIGURE 5. Tumor-to-blood ratios (%ID/g wet weight) at 4–4.5 hr postinjection for the various ^{67}Ga radiotracers studied. Each bar represents data from one animal. Group 1— ^{67}Ga -DF-folate; Group 2— ^{67}Ga -DF-folate in mice on high-folate diet; Group 3— ^{67}Ga -DF-folate administered with excess folic acid; Group 4— ^{67}Ga -DF-folate with chase dose of folate intravenously 1 hr prior to death; Group 5— ^{67}Ga -DF; Group 6— ^{67}Ga -citrate.

bearing KB tumors (Fig. 4, Group 1). The specific involvement of the folate receptor in mediating this uptake is demonstrated by the reduced tumor accumulation of ^{67}Ga -DF-folate in the mice that either received a blocking dose of intravenous folate (Group 3; $p \leq 0.05$) or that were fed normal (high folate) rodent chow (Group 2; $p \leq 0.1$). Some reduction of tumor ^{67}Ga -DF-folate was also apparent in the three mice that received a chase dose of folate intravenously 1 hr prior to death (Group 4; $p \leq 0.05$ relative to Group 1), apparently indicating that tumor levels of the ^{67}Ga -DF-folate tracer had not been completely internalized.

The other control experiments demonstrate that, as expected, ^{67}Ga -DF lacking the conjugated folate moiety shows no tumor affinity (Fig. 4 and Table 1, Group 5). This contrasts with the administration of ^{67}Ga -citrate, which provided higher tumor accumulation of ^{67}Ga than observed with ^{67}Ga -DF-folate (Fig. 4, Group 6). However, ^{67}Ga -DF-folate yields vastly superior tumor-to-background contrast than ^{67}Ga -citrate, due to more rapid tracer clearance from blood and other nontarget tissues such as liver and muscle (Table 2 and Fig. 5).

DISCUSSION

Overexpression of the folate receptor is a common characteristic of cell transformation, making tumor-selective drug targeting possible with folate-drug conjugates. Normal tissue such as the choroid plexus, placenta and proximal tubules of the kidney express low concentrations of the folate-receptor, while barely detectable levels may also be found in the lung and the thyroid (9,10,17,18). In contrast, FBP may be expressed in tumor cells at concentrations several orders of magnitude greater than normal tissue (11). In tumor cell cultures, folate-receptor-mediated endocytosis allows over 10^6 molecules of folate-conjugate to enter each cell per hour (6). Internalization of these folate-conjugates must occur via a receptor-mediated pathway, since the uptake is specific for the attached folate molecule; saturable at nanomolar concentrations; inhibited at low temperatures; competitively blocked by excess free folate or antibody to FBP; and eliminated by removal of FBP from the cell surface (6–12).

The present study was undertaken to evaluate tumor targeting with a radiolabeled ^{67}Ga -deferoxamine-folate conjugate in in-

tact animals and was based on previous experiments showing this material to exhibit folate receptor-mediated tumor cell uptake in vitro (29). The ^{67}Ga -DF-folate conjugate was synthesized for these studies as a convenient experimental prototype for the broad spectrum of radiopharmaceuticals that could be developed based on folate conjugates of low-molecular weight radiometal chelates. The deferoxamine chelator was specifically selected because it: (a) is commercially available and relatively inexpensive due to its clinical use in treating iron toxicity (34); (b) is known to bind the Ga^{3+} ion with high affinity (35–40), making commercially available ^{67}Ga a convenient gamma-emitting radiolabel; and (c) can be conveniently conjugated via its terminal $-\text{NH}_2$ group to the folate-targeting moiety.

Successful execution of the present study required an animal model that would mimic human neoplastic disease both in terms of the folate receptor content of the tumor and the free-folate concentration of the serum. As an initial animal model, we employed the athymic mouse implanted subcutaneously with human nasopharyngeal carcinoma (KB) cells known to overexpress the folate receptor. It is expected that the results obtained with this tumor model can be extrapolated to other human tumors known to similarly overexpress FBP (17–27).

Serum folate from normal dietary sources will directly compete with the radiolabeled folate conjugate for tumor cell uptake via the folate receptor pathway. In the current study this became a substantial concern, since the high folate level of normal rodent chow leads to mouse serum folate concentrations that far exceed those of human serum (Fig. 2). Thus, to avoid compromising the athymic mouse as a model for predicting the feasibility of tumor-selective radiopharmaceutical delivery in humans, the animals' dietary intake of folate was restricted prior to our radiotracer studies. After 3 wk on folate-free diet, mouse serum folate levels dropped to $25 \pm 7 \text{ nM}$ from the initial $720 \pm 260 \text{ nM}$ serum folate level when the animals were fed normal rodent chow (Fig. 2). We believe this dietary intervention to be a reasonable manipulation of the animal model, since the mice used for the reported radiopharmaceutical biodistribution studies in all cases would still have serum folate levels higher than the 9–14 nM folate concentration of normal human serum (32).

Excellent tumor targeting was observed in a pilot study with two tumor-bearing mice that were studied 45–46 hr following intravenous administration of the ^{67}Ga -DF-folate conjugate (Fig. 3). The limited data available from this pilot experiment stimulated a more comprehensive follow-up study in which the involvement of the folate receptor was more critically probed at a shorter 4–4.5 hr time point that would be of greater interest from the standpoint of a clinical imaging study (Tables 1 and 2). The tumor uptake of ^{67}Ga -DF-folate at 4 hr postinjection in Group 1 was significantly reduced ($p \leq 0.05$) by intravenous pre-administration of excess folate (Group 3), as well as by maintaining the animals on normal folate-rich rodent chow ($p \leq 0.1$). Thus, tumor uptake of the ^{67}Ga -DF-folate radiotracer clearly appears to be a receptor-mediated process.

The animals of Group 4 received a chase dose of folic acid intravenously 1 hr prior to sacrifice and also showed a significant reduction ($p \leq 0.05$) in tumor levels of tracer relative to Group 1 (Table 1 and Fig. 4). The finding of displaceable radiotracer in the animals from Group 4 suggests, unexpectedly, that at 3.5 hr postinjection some of the tumor-associated radiotracer had not been internalized. The animals in Group 5 show tumor uptake of ^{67}Ga that is 50-fold lower than seen in Group 1 (Table 1), confirming the expectation that the ^{67}Ga -

deferoxamine complex (^{67}Ga -DF) lacking the conjugated folate fragment would exhibit no tumor affinity.

The behavior of ^{67}Ga -citrate was also of interest as a control study, both because of its current clinical application in tumor imaging with ^{67}Ga and because it illustrates the tumor-targeting efficiency that would result if the ^{67}Ga -DF-folate conjugate, like ^{67}Ga -citrate, underwent rapid ligand exchange in plasma to form ^{67}Ga -transferrin (41–44). The ^{67}Ga -citrate tracer (Group 6, Fig. 4) affords approximately 2-fold higher tumor uptake of radiotracer than ^{67}Ga -DF-folate (Group 1); however, tumor-to-background contrast is vastly superior with ^{67}Ga -DF-folate (Fig. 5 and Table 2), due to the greater efficiency with which the FBP-targeted agent is cleared from most nontarget tissues (Table 1).

CONCLUSION

The reported results demonstrate the feasibility of radiopharmaceutical targeting to tumors via the folate receptor. The receptor-based tumor targeting observed with ^{67}Ga -DF-folate suggests that the folate receptor may be viable as a molecular target for a broader spectrum of tumor-directed folate-chelate conjugates in which the chelating agent and metal ion radiolabel can be manipulated to optimize radiopharmaceutical biodistribution, pharmacokinetics and nuclear properties.

ACKNOWLEDGMENTS

This work was supported by grants from the National Cancer Institute (RO1-CA46909) and TRASK Funds. The Purdue Athymic Mouse Facility is partially supported by Cancer Center (Core) Support grant #P30-CA23168 awarded by the National Cancer Institute.

REFERENCES

1. Anderson RGW, Kamen BA, Rothberg KG, et al. Potocytosis: sequestration and transport of small molecules by caveolae. *Science* 1992;255:410–411.
2. Forgac M. Structure and function of vacuolar class of ATP-driven pumps. *Physiological Rev* 1989;69:765–795.
3. Darnell JE. *Molecular Cell Biology*. San Francisco: W.H. Freeman; 1990:555–561.
4. Anderson RGW. The link between clathrin-coated pits and receptor mediated endocytosis. In: (Lonsdale-Eccles JD, ed.) *Protein traffic in parasites and mammalian cells: proceedings of a workshop held at the International Laboratory for Research on Animal Diseases*. Nairobi, Kenya: Majestic Printing Works; 1989:18–21.
5. Pastan I, Willingham MC. The pathway of endocytosis. In: Pastan I, Willingham MC, eds. *Endocytosis*. New York: Plenum Press; 1985:1–40.
6. Leamon CP, Low PS. Delivery of macromolecules into living cells: a method that exploits folate receptor endocytosis. *Proc Natl Acad Sci USA* 1991;88:5572–5576.
7. Leamon CP, Low PS. Cytotoxicity of momordin-folate conjugates in cultured human cells. *J Biol Chem* 1992;267:24966–24971.
8. Leamon CP, Low PS. Membrane folate binding proteins are responsible for the folate-protein conjugate endocytosis into cultured cells. *Biochem J* 1993;291:855–860.
9. Leamon CP, Pastan I, Low PS. Cytotoxicity of folate-Pseudomonas exotoxin conjugates towards tumor cells: contribution of translocation domain. *J Biol Chem* 1993;268:24847–24854.
10. Lee RJ, Low PS. Delivery of liposomes into cultured KB cells via folate receptor-mediated endocytosis. *J Biol Chem* 1994;269:3198–3204.
11. Leamon CP, Low PS. Selective targeting of malignant cells with cytotoxin-folate conjugates. *J Drug Targeting* 1994;2:101–112.
12. Turek JJ, Leamon CP, Low PS. Endocytosis of folate-protein conjugates: ultrastructural localization in KB cells. *J Cell Sci* 1993;106:423–430.
13. Antony AC, Kane MA, Portillo RM, et al. Studies of the role of a particulate folate-binding protein in the uptake of 5-methyltetrahydrofolate by cultured human KB cells. *J Biol Chem* 1985;260:14911–14917.
14. Henderson GB, Tsuji JM, Kumar HP. Mediated uptake of folate by a high-affinity binding protein in sublines of L1210 cells adapted to nanomolar concentrations of folate. *J Membrane Biol* 1988;101:247–258.
15. Pizzomo G, Cashmore AR, Moroson BA, et al. 5,10-Dideazatetrahydrofolic acid

- (DDATHF) transport in CCRF-CEM and MA104 cell lines. *J Biol Chem* 1993;268:1017–1023.
16. Sirotnak FM. Obligatory genetic expression in tumor cells of a fetal membrane property mediating folate transport: biological significance and implications for improved therapy of human cancer. *Cancer Res* 1985;45:3992–4000.
17. Weitman SD, Lark RH, Coney LR, et al. Distribution of the folate receptor GP38 in normal and malignant cell lines and tissues. *Cancer Res* 1992;52:3396–3401.
18. Miotti S, Canevari S, Menard S, et al. Characterization of human ovarian carcinoma-associated antigens defined by novel monoclonal antibodies with tumor-restricted specificity. *Int J Cancer* 1987;39:297–303.
19. Mezzanzanica D, Garrido MA, Neblock DS, et al. Human T-lymphocytes targeted against an established human ovarian carcinoma with a bispecific F(ab')₂ antibody prolong host survival in a murine xenograft model. *Cancer Res* 1991;51:5716–5721.
20. Rothenberg SP, DaCosta M. Further observations on the folate-binding factor in some leukemic cells. *J Clin Invest* 1971;50:719–726.
21. Westerhof GR, Jansen G, van Emmerik N, et al. Membrane transport of natural folates and antifolate compounds in murine L1210 leukemia cells: role of carrier- and receptor-mediated transport systems. *Cancer Res* 1991;51:5507–5513.
22. Coney LR, Tomasetti A, Carayannopoulos I, et al. Cloning of a tumor-associated antigen: MOv18 and MOv19 antibodies recognize a folate-binding protein. *Cancer Res* 1991;51:6125–6132.
23. Campbell IG, Jones TA, Foulkes WD, et al. Folate-binding protein is a marker for ovarian cancer. *Cancer Res* 1991;51:5329–5338.
24. Franklin WA, Waintrub M, Edwards D, et al. New anti-lung-cancer antibody cluster 12 reacts with human folate receptors present on adenocarcinoma. *Int J Cancer* 1994;8:89–95.
25. Mantovani LT, Miotti S, Menard S, et al. Folate binding protein distribution in normal tissues and biological fluids from ovarian carcinoma patients as detected by the monoclonal antibodies Mov18 and Mov19. *Eur J Cancer* 1994;30A:363–369.
26. Holm J, Hansen SI, Sondergaard K, Hoier-Madsen M. The high affinity folate binding protein in normal and malignant mammary gland tissue. *Chem Biol Pteridines and Folates* 1993;757–760.
27. Ross JF, Chaudhuri PK, Ratnam M. Differential regulation of folate receptor isoforms in normal and malignant tissue in vivo and in established cell lines. *Cancer* 1994;73:2432–2443.
28. Garin-Chesa P, Campbell I, Saigo PE, et al. Trophoblast and ovarian cancer antigen LK26: Sensitivity and specificity in immunopathology and molecular identification as a folate-binding protein. *Am J Pathol* 1993;142:557–567.
29. Wang S, Lee RJ, Mathias CJ, Green MA, Low PS. Synthesis, purification and tumor cell uptake of a potential radiopharmaceutical for tumor imaging: ^{67}Ga -deferoxamine-folate conjugate. *Bioconj Chem*: in press.
30. Bates RG, Vega CA, White DR. Standards for pH measurements in isotonic saline media of ionic strength $I = 0.16$. *Anal Chem* 1978;50:1295–1300.
31. McHugh M, Chang YC. Demonstration of a high affinity folate binder in human cell membrane and its characterization in cultured human KB cells. *J Biol Chem* 1979;254:11312–11318.
32. Kutsy RJ. *Handbook of vitamins, minerals and hormones*, 2nd ed. New York, NY: Van Nostrand Reinhold; 1981:273.
33. Samuels ML. *Statistics for the life sciences*. San Francisco, CA: Dellen Publishing; 1989:249–256.
34. Propper RD, Shurin SB, Nathan DG. Reassessment of the use of desferrioxamine B in iron overload. *N Eng J Med* 1976;294:1421–1423.
35. Weiner RE, Thakur ML, Goodman M, Hoffer PB. Relative stability of In-111 and Ga-67 desferrioxamine and human transferrin complexes. *Radiopharmaceuticals II*. New York, NY: Society of Nuclear Medicine; 1979:331–340.
36. Yokoyama A, Ohmomo Y, Horiuchi K, et al. Deferoxamine, a promising bifunctional chelating agent for labeling proteins with gallium: Ga-67 DF-HSA. *J Nucl Med* 1982;23:909–914.
37. Janoki AG, Harwig JF, Wolf W. Studies on high specific activity labeling of proteins using bifunctional chelates: Ga-67-DF-HSA. *Nucl Med Biol* 1982;1:689–692.
38. Koizumi M, Endo K, Kunimatsu M, et al. Preparation of ^{67}Ga -labeled antibodies using desferrioxamine as a bifunctional chelate, an improved method. *J Immunol Meth* 1987;104:93–102.
39. Vera DR. Gallium-labeled deferoxamine-galactosyl-neoglycoalbumin: a radiopharmaceutical for measurement of hepatic receptor biochemistry. *J Nucl Med* 1992;33:1160–1166.
40. Smith-Jones PM, Stoltz B, Bruns C, et al. Gallium-67/gallium-68-[DFO]-octreotide—a potential radiopharmaceutical for PET imaging of somatostatin receptor-positive tumors: synthesis and radiolabeling in vitro and preliminary in vivo studies. *J Nucl Med* 1994;35:317–325.
41. Harris WR, Pecoraro VL. Thermodynamic binding constants for gallium transferrin. *Biochemistry* 1983;22:292–299.
42. Larson SM. Mechanisms of localization of gallium-67 in tumors. *Sem Nucl Med* 1978;3:193–204.
43. Hoffer P. Gallium: mechanisms. *J Nucl Med* 1980;21:282–285.
44. Green MA, Welch MJ. Gallium radiopharmaceutical chemistry. *Nucl Med Biol* 1989;16:435–448.